Leakage Based Beam Shaping for Cooperative Communication in MANETs

Tim Rüegg*, Raphael T. L. Rolny†, Armin Wittneben*,
*ETH Zurich, Communication Technology Laboratory, 8092 Zurich, Switzerland
{rueegg,wittneben}@nari.ee.ethz.ch
†Armasuisse Science and Technology, 3602 Thun, Switzerland
raphael.rolny@armasuisse.ch

***Abstract*—Using the concepts of phased arrays, cooperative communication in military MANETs has the potential to strongly increase the transmission range while reducing the probability of being detected by hostile units. However, due to the random placement of the nodes and their potentially large separation, the standard pattern synthesis tools cannot be applied or require large computational complexity. In this context, we propose leakage based beam shaping, a low complexity pattern synthesis approach which minimizes the leakage power in undesired directions while maintaining coherent addition in the desired direction. We discuss the resulting signal power - leakage power trade-off and carefully investigate its potential and practical feasibility in military MANETs.**

I. Introduction

Modern wireless military networks are usually organized as mobile ad hoc networks (MANETs), where the pairwise communication between two nodes is done either with direct communication or with a multi hop scheme if the destination cannot be reached within a single hop [1]. While the direct communication has limited range, multi hop communication requires sophisticated routing and introduces a long delay (depending on the number of hops). Moreover, due to the clustered nature of military networks (organized in units, possibly spatially separated), two nodes might still be out of communication range, even with a multi hop transmission.

In order to avoid these drawbacks, multiple nodes could cooperate by forming a virtual antenna array (VAA) and optimize their radiation pattern analogously to phased arrays [2]. That is, they first exchange their transmit data and then jointly transmit the signal. This way, large gains in the radiated power can be achieved in the desired direction, leading to a larger communication range. Furthermore, by appropriate amplitude and phase excitation the radiated power in undesired directions can be minimized. This is useful to decrease the interference into the network and – in the context of military MANETs – can reduce the probability of being detected and localized by hostile units. To optimize the radiation pattern only the relative positions of the transmitting nodes to each other need to be available. No channel state information at the transmitter (CSIT) is required.

However, a virtual phased array of nodes in a MANET faces several practical challenges. Different to classical phased arrays where the elements are closely spaced to each other and uniformly arranged, the nodes in a military MANET are randomly placed and possibly separated by multiple wavelengths. This leads to spiky and non-regular array patterns. Moreover, the nodes have to be coordinated, synchronized (in time, frequency and phase) and exact (relative) position information needs to be available, which might be problematic due to the mobility of the nodes.

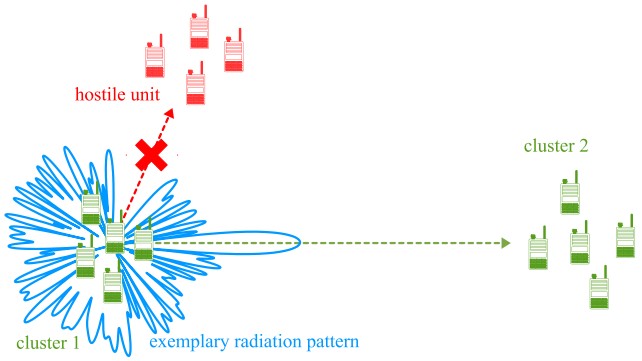

Fig. 1. Considered scenario for beam shaping: range extension in desired direction, singal suppression towards hostile untis.

In this paper, we consider a setup as shown in Fig. 1 and investigate the potential and practical challenges of cooperative communication in military MANETs. A node in cluster 1 wants to communicate over a large distance to a node in cluster 2. Using the concepts of phased arrays, the pattern shall be designed such that the range is extended, the signal power in the direction of the hostile units is suppressed, and the interference into the network is minimized.

Various pattern synthesis tools have been introduced for uniform linear arrays (ULAs) and uniform rectangular arrays (URAs), such as the Fourier transform method, the Dolph-Chebyshev synthesis and many others [2]. Furthermore, a large variety of adaptive array algorithms were proposed which allow for an arbitrary arrangement of the antennas [3]–[5]. However, while the tools for ULAs and URAs can not be applied in our setup due to the necessity of regularly arranged nodes (which is generally not the case in MANETs), the adaptive array algorithms are very complex and require a high computational complexity, which might be prohibitive in a military environment.

In this context, we propose leakage based beam shaping (LBBS), a low complexity pattern synthesis approach based

on the maximization of the signal-to-leakage ratio [6]. It minimizes the leakage power (signal power in undesired directions) while maintaining coherent addition in the desired direction. Hence, the transmission range can be extended while the interference into the network is minimized and the probability of being detected is reduced. We discuss the trade-off between the signal enhancement and the leakage suppression and thoroughly evaluate the proposed scheme. We furthermore address various practical considerations of LBBS in military networks.

II. System Setup and Pattern Synthesis

In the following, we are going to introduce the system setup of a cluster of cooperating nodes, the directivity of the antenna array for the performance evaluation, and finally the pattern synthesis. The scenarios and propagation environments in which the application of the proposed scheme is reasonable are discussed in Sec. IV-A.

We consider N_t nodes randomly distributed in a square of side length a centered around the origin, with $x_i, y_i \in [-\frac{a}{2}, \frac{a}{2}]$ the x- and y-coordinate of node i, $i \in \{1, \ldots, N_\mathrm{t}\}$. All nodes are assumed to be equipped with an identical, single, omnidirectional antenna. The minimum pairwise separation between the nodes is considered to be $\lambda/2$, with λ the wavelength, i.e. the antennas are uncoupled. Hence, the far field array factor in direction ϕ is given by

$$Y(\phi) = \sum_{i=1}^{N_\mathrm{t}} A_i e^{-j\xi_i} e^{-j\frac{2\pi}{\lambda} d_i(\phi)} \quad (1)$$

$$= \bar{\mathbf{h}}\mathbf{w}, \quad (2)$$

where $d_i(\phi) = (\cos\phi \cdot x_i + \sin\phi \cdot y_i)$ denotes the path length difference of node i with respect to the origin, A_i the amplitude excitation and ξ_i the phase excitation of node i, summarized into the weight vector

$$\mathbf{w} = \left[A_1 e^{-j\xi_1}, \ldots, A_{N_\mathrm{t}} e^{-j\xi_{N_\mathrm{t}}}\right]^\mathsf{T} \quad (3)$$

and the steering vector

$$\bar{\mathbf{h}} = \left[e^{-j\frac{2\pi}{\lambda} d_1(\phi)}, \ldots, e^{-j\frac{2\pi}{\lambda} d_{N_\mathrm{t}}(\phi)}\right]. \quad (4)$$

As we consider omnidirectional antennas, the radiation pattern of the antenna array is given as the radiation pattern of a single antenna multiplied with the array factor. Hence, the gain in radiated power compared to an omnidirectional antenna is given as

$$D(\phi) = |Y(\phi)|^2. \quad (5)$$

A. Leakage Based Beam Shaping

As discussed in the introduction, the goal is to extend the transmission range in the desired direction ϕ_s, suppress the leakage into the direction of hostile units, and minimize the interference into the network. To this end, we consider a desired beam width ψ_s (centered around the desired direction ϕ_s) in which no leakage suppression is applied. To quantify the power leaking into all other directions, we introduce M undesired directions $\phi_{\mathrm{l},m}$, $m \in \{1, \ldots, M\}$, uniformly spaced outside of the desired beam width. We furthermore introduce a sector L of width ψ_l centered around ϕ_L in which we strongly want to suppress the leakage (as e.g. hostile units are assumed to be in this direction). This setup is shown in Fig. 2.

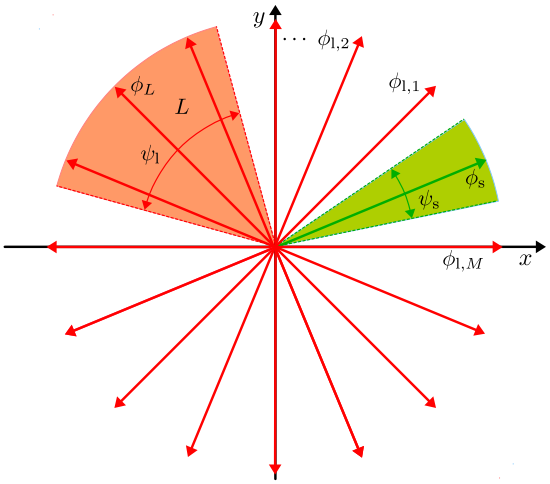

Fig. 2. Setup for leakage based beam shaping: one desired direction ϕ_s with beam width ψ_s and M undesired directions $\phi_{\mathrm{l},m}$, $m \in \{1, \ldots, M\}$ with a special emphasis on the sector L of width ψ_l centered around ϕ_L.

Analogously to (4) we can state the channel (steering vector) in the desired direction as

$$\bar{\mathbf{h}}_\mathrm{s} = \left[e^{-j\frac{2\pi}{\lambda} d_1(\phi_\mathrm{s})}, \ldots, e^{-j\frac{2\pi}{\lambda} d_{N_\mathrm{t}}(\phi_\mathrm{s})}\right], \quad (6)$$

and the channels in the undesired directions as

$$\bar{\mathbf{h}}_{\mathrm{l},m} = \left[e^{-j\frac{2\pi}{\lambda} d_1(\phi_{\mathrm{l},m})}, \ldots, e^{-j\frac{2\pi}{\lambda} d_{N_\mathrm{t}}(\phi_{\mathrm{l},m})}\right], \quad (7)$$

$m \in \{1, \ldots, M\}$. The channel into all undesired directions can then be summarized as

$$\mathbf{H}_\mathrm{l} = \mathrm{diag}(c_1, \ldots, c_M) \cdot \begin{bmatrix} \bar{\mathbf{h}}_{\mathrm{l},1} \\ \vdots \\ \bar{\mathbf{h}}_{\mathrm{l},M} \end{bmatrix}. \quad (8)$$

The weights c_m with $m \in \{1, \ldots, M\}$ are used to emphasize the leakage in the sector L. Thereby, $c_m = 1$, if the direction $\phi_{\mathrm{l},m}$ is outside of L and $c_m = c$ (the suppression factor) if it is inside L. The bigger c, the stronger is the leakage suppression inside sector L. A straight forward extension is to assign arbitrary c_m to weight the different undesired directions individually. With this, e.g., multiple sectors can be realized or the weighting between suppression sector L and other directions can be traded off.

Note that the channels $\bar{\mathbf{h}}_\mathrm{s}$ and $\mathbf{H}_\mathrm{l}$ do not contain any information about the specific channel characteristics like fading or path loss, as we do not consider to have this information available. It only includes the radiation pattern in the far field. Hence, there is no point in introducing any signal or leakage power constraint for the optimization of the weight vector $\mathbf{w}$.

Instead, we rather maximize the signal-to-leakage power ratio as introduced in [6]. Considering Gaussian transmit symbols $s \sim \mathcal{CN}(0, 1)$, the signal power (power dissipated in the desired direction) can be stated as

$$P_\mathrm{s} = \mathbf{w}^\mathsf{H} \bar{\mathbf{h}}_\mathrm{s}^\mathsf{H} \bar{\mathbf{h}}_\mathrm{s} \mathbf{w}, \quad (9)$$

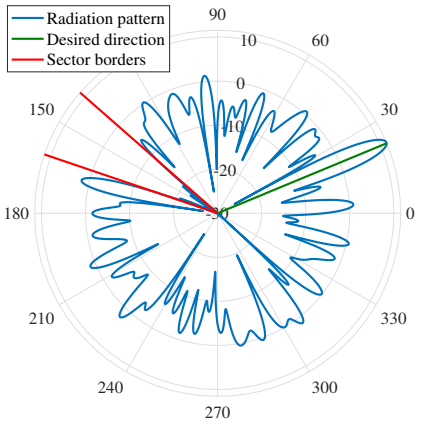

Fig. 3. Exemplary radiation pattern [dBi] of LBBS for $N_\mathrm{t} = 25$, $a = 10\lambda$, $\psi_\mathrm{l} = 22.5°$, and $c = 10$.

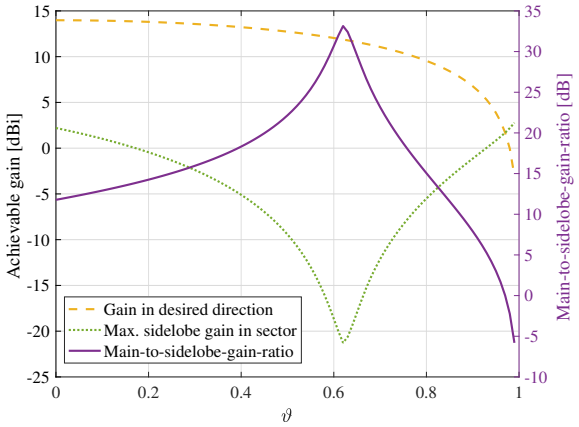

Fig. 4. Transmit power - leakage power trade-off corresponding to the radiation pattern in Fig. 3.

and the total weighted leakage power (weighted power dissipated in undesired directions) as

$$P_\mathrm{l} = \mathbf{w}^\mathsf{H}\mathbf{H}_\mathrm{l}^\mathsf{H}\mathbf{H}_\mathrm{l}\mathbf{w}. \tag{10}$$

The optimization problem can then be stated as

$$\hat{\mathbf{w}} = \arg\max_{\mathbf{w}} \frac{\mathbf{w}^\mathsf{H}\bar{\mathbf{h}}_\mathrm{s}^\mathsf{H}\bar{\mathbf{h}}_\mathrm{s}\mathbf{w}}{\mathbf{w}^\mathsf{H}\mathbf{H}_\mathrm{l}^\mathsf{H}\mathbf{H}_\mathrm{l}\mathbf{w}}, \quad \text{s.t.} \quad \mathbf{w}\mathbf{w}^\mathsf{H} = 1. \tag{11}$$

The normalization of the transmit power to 1 is done to compare the resulting array pattern to a single isotropic antenna transmitting at unit power. The transmit power can finally be scaled to any desired value. The optimal $\hat{\mathbf{w}}$ can be found as a scaled version of the eigenvector corresponding to the largest eigenvalue of the generalized eigenvalue decomposition of $\bar{\mathbf{h}}_\mathrm{s}^\mathsf{H}\bar{\mathbf{h}}_\mathrm{s}$ and $\mathbf{H}_\mathrm{l}^\mathsf{H}\mathbf{H}_\mathrm{l}$ as shown in [6]. Hence, no iterative optimization is necessary and only low computational complexity is required.

An exemplary radiation pattern for $N_\mathrm{t} = 25$, $a = 10\lambda$, $\psi_\mathrm{s} = 5$ degree, $\psi_\mathrm{l} = 25$ degree, $c = 10$, and $M = 5000$ can be found in Fig. 3. While the signal in the desired direction is amplified ($+11.9$ dBi), the leakage in the sector is strongly suppressed (maximal side lobe gain: -21.8 dBi), decreasing the probability of being detected. As can be seen, the pattern is non-regular and spiky. This comes from the random node placement and the large separation between the nodes (further discussed in Sec. III).

B. The Signal Power - Leakage Power Trade-Off

As shown in [7], the weight vector $\mathbf{w}$ can be separated into a signal term $\mathbf{w}_\mathrm{s}$, shaping the signal in the desired direction, and a compensation term $\mathbf{w}_\mathrm{c}$ minimizing the leakage in an orthogonal subspace without affecting the signal term:

$$\mathbf{w} = \mathbf{w}_\mathrm{s} + \mathbf{w}_\mathrm{c}. \tag{12}$$

That is, the directivity in the desired direction is only determined by the signal term. It can be found as $\mathbf{w}_\mathrm{s} = \mathbf{u}\mathbf{u}^\mathsf{H}\mathbf{w}$, the projection of $\mathbf{w}$ onto the subspace of the channel in the desired direction, with $\mathbf{u}$ the basis vector of $\bar{\mathbf{h}}_\mathrm{s}$ (i.e. a scaled version of $\bar{\mathbf{h}}_\mathrm{s}$). The compensation term is then given as $\mathbf{w}_\mathrm{c} = \mathbf{w} - \mathbf{u}\mathbf{u}^\mathsf{H}\mathbf{w}$.

The signal term maximizing (11) can be found as a scaled version of $\bar{\mathbf{h}}_\mathrm{s}^\mathsf{H}$ leading to coherent addition of the signal components in the desired direction. However, due to the leakage reduction, the available transmit power is distributed onto $\mathbf{w}_\mathrm{s}$ and $\mathbf{w}_\mathrm{c}$. Thus, not the full gain of coherent combining can be achieved in the desired direction. That is, reducing the leakage power is traded-off for lower signal power in the desired direction, resulting in a smaller gain in the transmission range.

By normalizing the signal and the compensation term to unit power, resulting in $\tilde{\mathbf{w}}_\mathrm{s}$ and $\tilde{\mathbf{w}}_\mathrm{c}$, and weighting them according to

$$\tilde{\mathbf{w}} = \sqrt{1-\vartheta^2} \cdot \tilde{\mathbf{w}}_\mathrm{s} + \vartheta \cdot \tilde{\mathbf{w}}_\mathrm{c}, \tag{13}$$

with $\vartheta \in [0, 1]$, the trade-off between signal power and leakage power can be controlled. Any signal power level between coherent combining with no leakage suppression ($\vartheta = 0$) and no signal at all ($\vartheta = 1$) can be achieved. Hence, depending on the necessary gain for the range extension in the desired direction, the leakage can be minimized by adjusting ϑ.

In Fig. 4 the transmit power - leakage power trade-off corresponding to the radiation pattern in Fig. 3 is illustrated. We thereby consider the achievable power gain in the desired direction, the maximal side lobe gain in the sector L and the ratio of these two gains. The optimal trade-off for the main-to-sidelobe-gain-ratio is clearly visible at $\vartheta \approx 0.62$. By decreasing ϑ, the signal power is increased at the price of strongly increasing leakage power in the sector, reducing the gain ratio. Increasing ϑ above 0.62 does not make sense, as the signal power is decreased while the leakage power in the sector L increases again.

The only way to further decrease the leakage power in the sector is to increase the suppression factor c. This factor strongly affects the performance of LBBS. For a higher c, the leakage in the sector is suppressed more strongly. However, as for larger c the compensation term requires a higher share of the total transmit power, the achievable gain in the desired direction is decreased.

Hence, the trade-off between desired signal power and leakage suppression can be controlled in two different ways:

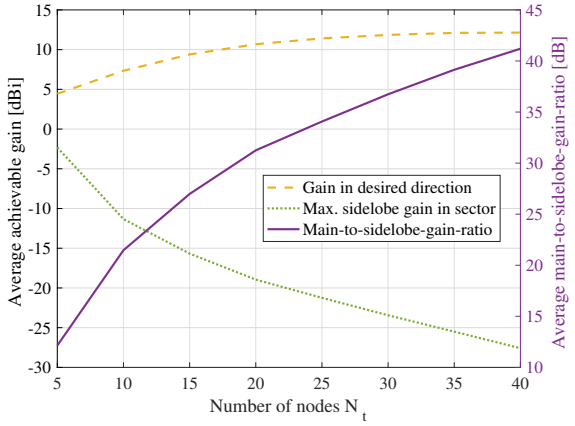

Fig. 5. Performance of LBBS for $a = 10\lambda$ and $\psi_l = 22.5°$ and $c = 10$.

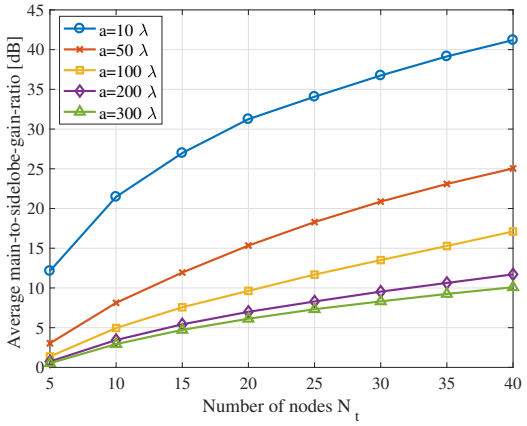

Fig. 6. Main-to-side-lobe-gain-ratio of LBBS for $\psi_l = 22.5°$ and $c = 10$.

by adapting c and by varying ϑ. Choosing c large and then varying ϑ such that the desired trade-off is achieved allows for large ranges of the signal and leakage power. However, if no optimization of the trade-off is desired or required, c can be chosen such that on average the desired gains are achieved.

III. Performance Evaluation

In the following, we are going to evaluate the proposed LBBS for varying cluster size a, number of cooperating nodes N_t, and sector width ψ_l, by considering the solution of (11) as the weight vector. That is, we choose the leakage minimizing ϑ. The desired direction is set to $\phi_\mathrm{s} = 25$ degree with $\psi_\mathrm{s} = 5$ degree, the sector L is centered around $\phi_L = 150$ degree, and $M = 5000$ undesired directions are considered. The suppression factor is set to $c = 10$. 1000 Monte Carlo simulations were performed and the results averaged.

In Fig. 5 the resulting average achievable gain in the desired direction, the average maximal sidelobe gain in the sector, and the resulting average achievable main-to-sidelobe-gain-ratio is shown for $a = 10\lambda$ and $\psi_l = 22.5$ degree. Already for a relatively small number of nodes, $N_\mathrm{t} = 5$, the leakage in the sector can be efficiently suppressed, while a gain of 5 dBi in the desired direction is achieved. For increasing number of cooperating nodes the performance strongly increases. As more degrees of freedom are available, very low leakage levels are achieved at high gains in the desired direction. Hence, the transmission range can be strongly increased while the probability of being detected is decreased. However, the achievable performance is strongly affected by the cluster size a and the sector width ψ_l as shown in the following.

As seen in Fig. 3, the radiation pattern is irregular and very spiky due to the randomness of the node location and their spatial separation. The number of peaks in the pattern even further increases with increasing spatial separation of the nodes. This can be seen in Tab. I which lists the average number of peaks in the radiation pattern for various cluster sizes and number of nodes. While the number of nodes N_t only has a small impact, the average number of peaks is strongly affected by the side length a.

TABLE I
Average number of peaks in radiation pattern (rounded).

N_t	$a = 10\lambda$	$a = 50\lambda$	$a = 100\lambda$	$a = 200\lambda$	$a = 300\lambda$
5	38	187	368	740	1106
40	42	208	413	818	1216

The increasing number of peaks in the pattern has a strong impact on the beam shaping. Due to the increased number of peaks more leakage has to be suppressed, leading to reduced main-to-side-lobe-gain-ratios for large cluster sizes. This is visualized in Fig. 6, which shows the resulting average main-to-side-lobe-gain-ratio for varying cluster size and $\psi_l = 22.5$ degree. The achievable gain-ratio strongly decreases for increasing cluster size. This, however, can be compensated with an increased number of cooperating nodes.

While the cluster size a has a very strong impact on the achievable performance, the impact of the sector width ψ_l is smaller. This can be seen in Fig. 7 which shows the average main-to-side-lobe-gain-ratio for varying sector width ψ_l and fixed side length $a = 10\lambda$. Obviously, the gain is decreasing for large sector widths, as more leakage needs to be suppressed. However, especially for a large N_t, the degradation from a sector width of 11.25 degree to 90 degree is rather small. Hence, even if the direction of the hostile units is only known with a large uncertainty and the sector width has to be chosen large (or if multiple hostile units in a large sector have to be suppressed) still large gains in the transmission range can be achieved.

IV. Practical Considerations

As shown above, LBBS has a huge potential to increase the transmission range while decreasing the leakage into the network at low computational complexity. In practice however, various factors impact the performance and have to be considered. In the following, we are going to discuss several such practical aspects and limitations of LBBS.

A. Propagation Environment

Throughout the paper we considered the radiation pattern of the antenna array for the performance evaluation. It indicates

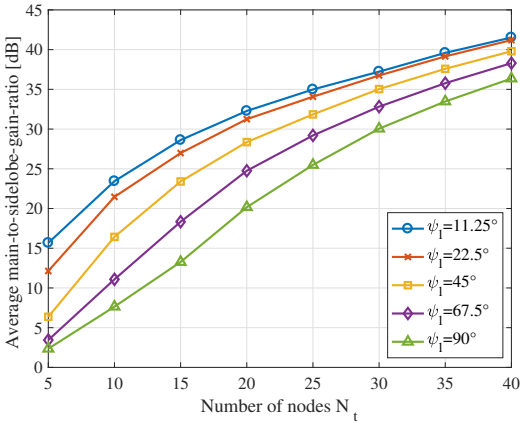

Fig. 7. Main-to-side-lobe-gain-ratio of LBBS for $a = 10\lambda$ and $c = 10$.

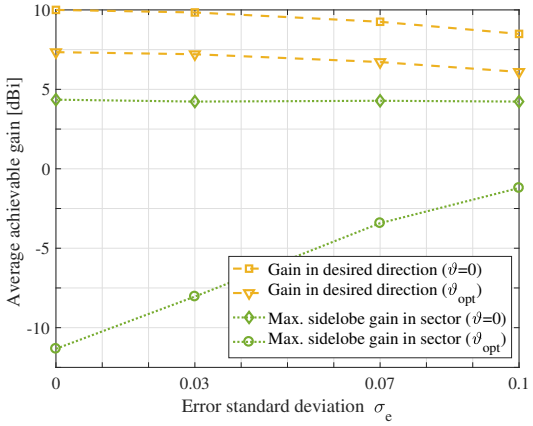

Fig. 8. Impact of erroneous location information on the achievable gains.

the gain in radiated power compared to an isotropic radiator in free space at large distance. That is, to achieve the predicted gains in the desired direction, the transmit cluster should see the destination under a low angular spread in the desired direction, such that focusing the energy in this direction is reasonable.

Thereby, scatterers impact the predicted gains due to constructive or destructive addition of the signal at the destination. However, if the maximal gain of the radiation pattern is achieved in the desired direction, the impact of a scatterer is decreased, as its contribution is scaled according to the array pattern. That is, while for a constructive scatterer a smaller gain is achieved, a destructive scatterer leads to a larger gain of LBBS compared to an isotropic radiator.

A scatterer could also have a significant impact on the signal power at a hostile unit. While the leakage is minimized in the sector L, a scatterer outside of the sector could reflect signal energy to the hostile units. If the reflected signal is strong enough, detection is possible. However, if the direction of the scatterers is known, multiple sectors can be realized to suppress the leakage power also in their directions or, in rich scattering environments, the whole leakage can be minimized by setting $c = 1$.

Ideally, the transmit array would be on an elevated position (e.g. on a hill), with a LOS to the destination. Furthermore, the separation between the source and the destination has to be large, such that the assumption holds that each transmitter sees the destination under the same angle.

B. Location Information

For beam shaping, no channel state information (CSI) is required. The only information needed is the relative position of the transmitting elements to each other (c.f. above) and the position of the destination (or at least the direction to it). The relative position information can be acquired in various forms. Three eligible technologies are described in the following:

- **Satellite based localization:** To localize the nodes within the cluster, satellite based localization such as GPS or differential GPS technology can be used. In combination with measurements from inertial measurement units (IMUs) a location accuracy in the order of centimeters can be achieved [8].
- **Self-calibration:** In this case, the nodes try to calibrate themselves on their own using e.g. ultra-wideband (UWB) technology. In [9], e.g., an algorithm for self-calibration is suggested, with which an accuracy in the order of centimeters can be achieved.
- **External calibration:** In this case, there are different (terrestrial) nodes far from the transmit cluster which orchestrate the localization process, e.g. based on angle of arrival estimation (AoA). High accuracy can be achieved with sophisticated algorithms [10].

All these technologies can lead to high accuracy. Nevertheless, non of them can determine the location information perfectly. Thus, we are going to investigate the impact of erroneous location information in the following, considering

$$\tilde{x}_i = x_i + e_{x,i}, \tag{14}$$

$$\tilde{y}_i = y_i + e_{y,i} \tag{15}$$

with

$$e_{x,i}, e_{y,i} \overset{\text{i.i.d}}{\sim} \mathcal{N}(0, \sigma_\text{e}^2) \quad \text{for } i = 1, \ldots, N_\text{t} \tag{16}$$

the error terms. The standard deviation of the error is set to $\sigma_\text{e} \in \{0, 0.03, 0.07, 0.1\} \cdot \lambda$. For a transmit frequency of 100 MHz (reasonable for military networks), i.e. $\lambda = 3$ m, $\sigma_\text{e} = 0.1\lambda$ corresponds to $\approx 95\%$ of the values inside ± 0.6 m of the original x and y position. For $\sigma_\text{e} = 0.03\lambda$ roughly 95% of the values are inside ± 0.2 m.

The resulting average gain in the desired direction, as well as the average maximal side lobe gain in sector L are shown in Fig. 8 for $N_\text{t} = 10$, $a = 10\lambda$, $\psi_L = 22.5$ degree and $c = 10$. While the loss in the achievable gain in the desired direction is less than 2 dB for $\sigma_e = 0.1\lambda$ for both, the standard LBBS (ϑ_opt) and coherent combining ($\vartheta = 0$), the increase of the maximal side lobe level in the sector L is drastic, even for a very low standard deviation of $\sigma_e = 0.03\lambda$. That is,

TABLE II
AVERAGE 3DB BEAM WIDTH FOR $N_\mathrm{t} = 10$ AND $\psi_l = 22.5$ DEGREE.

N_t	$a = 10\lambda$	$a = 50\lambda$	$a = 100\lambda$	$a = 200\lambda$	$a = 300\lambda$
10	$6.11°$	$1.29°$	$0.64°$	$0.32°$	$0.23°$

the leakage suppression is very sensitive to erroneous position information. Nevertheless, it is still possible to suppress the leakage below the level of an isotropic radiator (0 dBi). Furthermore, compared to the coherent combining ($\vartheta = 0$) where no leakage is suppressed, still significant gains can be achieved.

C. Synchronization

The synchronization of the nodes in time, frequency and phase is crucial. While the time and frequency synchronization are assumed to be available with a sufficient accuracy in a military MANET, accurate phase synchronization is challenging. Without proper synchronization, the performance suffers strongly, as shown in the following.

An erroneous phase synchronization has the same impact on the performance as erroneous location information. Both lead to a phase offset in the steering vector. More specifically, a zero mean Gaussian distributed phase error with standard deviation $\sigma_\theta = \frac{2\pi}{\lambda} \cdot \sigma_e$ has the same impact on the performance as a zero mean Gaussian distributed location error in x-direction with standard deviation σ_e. That is, for $\sigma_\theta = 2\pi \cdot 0.1 = 0.628$ (i.e. 95% of the phase errors are within ± 1.2 rad) we get the same performance degradation as for a position error with $\sigma_e = 0.1\lambda$ (c.f. Fig. 8).

D. Beam Width

As seen in Sec. III the number of peaks in the radiation pattern is strongly increasing with increasing cluster size. This also impacts the 3 dB beam width of the radiation pattern as shown in Tab. II for $N_\mathrm{t} = 10$ and $\psi_l = 22.5$ degree. The more peaks, the smaller is the average width of each peak. Already for a side length of $a = 50\lambda$ the average 3dB beam width decreases from over 6 degree for $a = 10\lambda$ down to 1.29 degree. That is, although large gains can be achieved in the desired direction, the location information of the destination, respectively the desired direction has to be known very accurately in order to achieve these gains.

A straight forward way to widen the beam width is to introduce multiple desired directions $\phi_{\mathrm{s},j}$, $j \in \{1, \ldots, J\}$, in ψ_s, leading to a matrix $\mathbf{H}_\mathrm{s}$ for the desired channel. The weight vector $\mathbf{w}$ can then be found analogously to (11) by replacing $\bar{\mathbf{h}}_\mathrm{s}$ with $\mathbf{H}_\mathrm{s}$. Depending on the number of desired directions and their spacing, the beam width can be strongly increased.

E. Bandwidth

In beam shaping, the radiation pattern is optimized for one specific frequency f_c (the center frequency of the transmit signal). Nevertheless, for reasonable bandwidths of the transmit signal, the degradation of the achievable gains are negligible. To see that, we consider the lower end of the VHF band (30 MHz) and a bandwidth of 25 kHz. That is, cenetred around f_c we have a maximal offset of $\Delta f = \pm 12.5$ kHz. This leads to an offset in the wave length of $\Delta\lambda = \pm 0.0042$ m $= \pm 0.00042\lambda$. From this number, it can be seen that the impact of this offset onto the steering vector is negligibly small.

F. Orientation of Antennas

Throughout the paper we considered the antenna pattern of all transmitting nodes to be the same. However, if, e.g., a dipole antenna of a mobile unit is not perfectly vertically positioned, its radiation pattern changes. Nevertheless, this would only have an impact on the amplitude of the received signal and not on the phase. While the leakage suppression could strongly suffer from that (if the differences in the radiation patterns of the antennas are large), the coherent addition in the desired direction is still obtained.

V. CONCLUSIONS AND OUTLOOK

In this paper, we introduced leakage based beam shaping, a low complexity pattern synthesis approach which minimizes the leakage in undesired directions while maintaining coherent addition in the desired direction. Due to its low computational complexity and the ability to deal with random node placements, it is well suited for user cooperation in military MANETs. By carefully evaluating the resulting signal power - leakage power trade-off, it has been shown that large gains in the transmission range can be achieved while the interference into the network is minimized and the probability of being detected by hostile units can significantly be reduced.

VI. ACKNOWLEDGMENT

This work was partially funded by the Swiss federal office for defense procurement, *armasuisse Science and Technology*.

REFERENCES

[1] J. Loo, J. Mauri, and J. Ortiz, *Mobile Ad Hoc Networks*. Auerbach Publications, 2012.
[2] R. J. Mailloux, *Phased Array Antenna Handbook*. Artech House, 2005.
[3] C. A. Olen and J. R. T. Compton, "A numerical pattern synthesis algorithm for arrays," *IEEE Transactions on Antennas and Propagation*, vol. 38, no. 10, pp. 1666–1676, October 1990.
[4] P. Y. Zhou and M. A. Ingram, "Pattern synthesis for arbitrary arrays using an adaptive array method," *IEEE Transactions on Antennas and Propagation*, vol. 47, no. 5, pp. 862–869, May 1999.
[5] R. L. Haupt, "Adaptive antenna arrays using a genetic algorithm," in *IEEE Mountain Workshop on Adaptive and Learning Systems*, July 2006.
[6] M. Sadek, A. Tarighat, and A. Sayed, "A leakage-based precoding scheme for downlink multi-user MIMO channels," *IEEE Trans. on Wireless Communications*, vol. 6, no. 5, pp. 1711–1721, 2007.
[7] T. Rüegg, A. U. T. Amah, and A. Wittneben, "On the trade-off between transmit and leakage power for rate optimal MIMO precoding," in *IEEE International Workshop on Signal Processing Advances in Wireless Communications (SPAWC)*, June 2014.
[8] S. Zhao, Y. Chen, and J. A. Farrell, "High-precision vehicle navigation in urban environments using an MEM's IMU and single-frequency GPS receiver," *IEEE Transactions on Intelligent Transportation Systems*, vol. 17, no. 10, pp. 2854–2867, Oct 2016.
[9] Z. W. Mekonnen and A. Wittneben, "Self-calibration method for TOA based localization systems with generic synchronization requirement," in *IEEE ICC 2015, London, UK*, Jun. 2015.
[10] A. J. Weiss and B. Friedlander, "Array shape calibration using sources in unknown locations-a maximum likelihood approach," *IEEE Transactions on Acoustics, Speech, and Signal Processing*, vol. 37, no. 12, pp. 1958–1966, Dec 1989.